

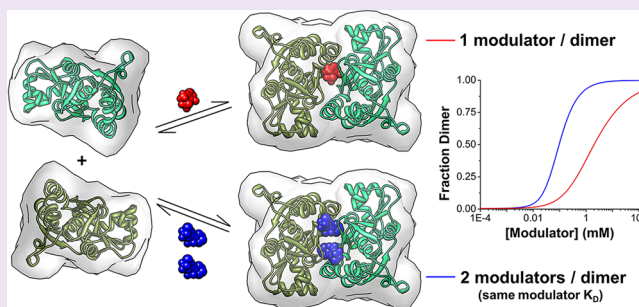
Role of Stoichiometry in the Dimer-Stabilizing Effect of AMPA Receptor Allosteric Modulators

Christopher P. Ptak,[†] Ching-Lin Hsieh,[‡] Gregory A. Weiland,[†] and Robert E. Oswald^{*,†}

[†]Department of Molecular Medicine and [‡]Department of Population Medicine and Diagnostic Sciences, College of Veterinary Medicine, Cornell University, Ithaca, New York 14853, United States

S Supporting Information

ABSTRACT: Protein dimerization provides a mechanism for the modulation of cellular signaling events. In α -amino-3-hydroxy-5-methyl-4-isoxazole-propionic acid (AMPA) receptors, the rapidly desensitizing, activated state has been correlated with a weakly dimeric, glutamate-binding domain conformation. Allosteric modulators can form bridging interactions that stabilize the dimer interface. While most modulators can only bind to one position with a one modulator per dimer ratio, some thiazide-based modulators can bind to the interface in two symmetrical positions with a two modulator per dimer ratio. Based on small-angle X-ray scattering (SAXS) experiments, dimerization curves for the isolated glutamate-binding domain show that a second modulator binding site produces both an increase in positive cooperativity and a decrease in the EC_{50} for dimerization. Four body binding equilibrium models that incorporate a second dimer-stabilizing ligand were developed to fit the experimental data. The work illustrates why stoichiometry should be an important consideration during the rational design of dimerizing modulators.



Protein–protein interactions (PPIs) play a key role in macromolecular assembly, signal recognition, and stabilization of functionally important conformational states¹ and have broad medical potential as targets of rationally designed therapeutics. Protein dimerizers are being developed that enhance existing weak PPIs or that create new PPIs.² A number of clinically promising dimerizers have been designed to induce PPIs including antibody-recruiting ligands for use in anticancer vaccines (heterodimers)³ and receptor activators for targeted gene therapies (hetero- and homodimers).² The symmetrical interfaces of protein homodimers offer a simple model for studying the basic principles of how small molecules can enhance dimerization at weak PPIs for use as allosteric regulators.

Of significance to brain chemistry, ionotropic glutamate receptors (iGluRs) contain dimeric ligand-binding domains (LBDs)^{4,5} within a multidomain architecture (Figures 1A and B).⁶ Dimerization of the LBD is critical to iGluR function. Following ligand-gated ion channel activation, the α -amino-3-hydroxy-5-methyl-4-isoxazole-propionic acid (AMPA) iGluR subtype rapidly desensitizes leading to channel closure.⁷ Desensitization has been linked to disruption of the dimer interface between GluA2 LBDs, while stabilization of a symmetrical dimer interface by a mutation (L483Y) reduces desensitization.⁵ Dimerization of the isolated LBD has a weak (mM) equilibrium constant and is a correlate of the short-lived activated-state. Small molecules interact with the LBD dimer interface and stabilize dimerization. In the full receptor, they slow desensitization, thereby acting as positive allosteric modulators. AMPA receptor-positive allosteric modulators

enhance learning and memory in rats and are therefore being explored as drug candidates for cognitive enhancement and in the treatment of autism.^{8–10}

The GluA2 LBD dimer interface forms a large symmetrical cavity that can bind allosteric modulators. The binding positions for three chemically distinct allosteric modulator classes vary along the interface but invariably increase the number of contacts that bridge the dimer.^{11–13} The extent of the modulator-binding pocket can be visually depicted using a modulator-accessible volume and further divided into 5 subsites (A, B, B', C, C') (Figure 1C).¹¹ Most of the modulators occupy the central portion of the cleft (A subsite) and bind with a stoichiometry of 1 modulator/dimer. Modulators in the thiazide class bind with a stoichiometry of 2 modulators/dimer. When one cyclothiazide (CYTZ) binds to the B and C subsites, a second can still bind to the identical B' and C' subsites (Figure 1D).⁵ The decrease in the size of the substituent at the thiazide 3'-position is linked to rotation of the thiazide by 40° into the hydrophobic C subsites.¹¹ The reorientation is associated with a shift into the A subsite, which results in the occlusion of second-site binding when the thiazide 7'-position is large (e.g., hydroflumethiazide (HFMZ); Figure 1E). Here, we study differences in the LBD-dimerizing ability of thiazides with stoichiometries of 1 versus 2 modulator/dimer.

Received: September 17, 2013

Accepted: October 23, 2013

Published: October 23, 2013

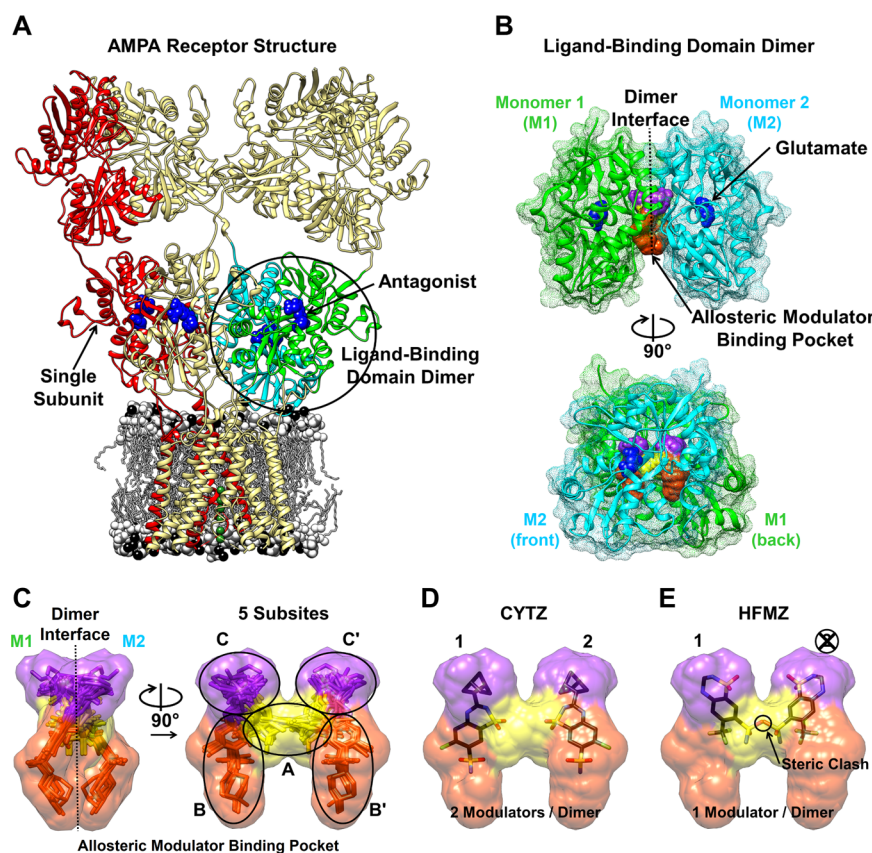


Figure 1. Ionotropic glutamate receptor structure [PDB: 3KG2].⁶ (A) The ligand-binding domain (LBD) from 2 subunits (green and cyan) forms a dimer. (B) The LBD dimer [PDB: 1FTJ]⁴ has 2 agonist-binding sites (blue) and a symmetrical allosteric modulator-binding pocket that extends along the dimer interface. The accessible volume of the modulator-binding cavity is depicted by surfacing a composite of bound modulator structures (see Supporting Information). (C) The modulator-binding pocket can be divided into 5 subites, A (yellow), B (orange), B', C (purple), and C'. (D) Cyclothiazide (CYTZ) binds at two sites in the modulator-binding pocket with 2-fold symmetry. (E) Hydroflumethiazide (HFMZ) binding extends into the A subsite, obstructing the second binding site and allowing only 1 HFMZ to bind per dimer.

A specific dimeric conformation of the GluA2 LBD is directly related to the activated state of the receptor. Understanding how allosteric modulators influence the equilibrium constants associated with dimerization is therefore important. Equilibrium cyclical models describing the degree of dimerization as a function of modulator concentration (in terms of receptor, R, and modulator, L) were created for both 1 and 2 modulator/dimer binding (Figure 2). The models consider that either dimerization (R_2) or modulator-binding (RL) can occur first in the path to the modulator-bound dimer (R_2L or R_2L_2). While we know from the structure that each thiazide binds with

distinct interactions to opposite halves of the dimer, we simplified the two models by assuming that one receptor–ligand complex (RL) structure is preferred. Still, the 1 modulator/dimer model contains 4 equilibrium constants (Figure 2A); the 2 modulator/dimer model requires 6 equilibrium constants (Figure 2B).

A range of techniques offer the potential to characterize the oligomeric state of proteins. Small angle X-ray scattering (SAXS) is a robust method that allows for the ability to distinguish between components in mixtures.¹⁴ SAXS can detect the subtle differences in GluA2 LBD structure associated with agonist and antagonist binding.¹⁵ Here, SAXS was used to produce distinct scattering curves for the monomeric and dimeric GluA2 LBD (Figure 3A). Based on theoretical scattering curves (CRY SOL)¹⁶ for the monomer and dimer (PDB: 1FTJ),⁴ the fraction of dimer present was near zero for the GluA2 LBD, consistent with its weak association constant, and 0.99 for the nondesensitizing L483Y mutant.¹⁶ Low-resolution envelopes derived from these curves correspond to the volume expected for the monomeric and dimeric GluA2 LBD (Figure 3B).

SAXS scattering curves for GluA2 LBD were collected in the presence of allosteric modulators. We examined the effect of 3 modulators, CYTZ, HFMZ, and trichlormethiazide (TCMZ), on LBD dimerization. Based on structural studies, CYTZ and TCMZ bind to two symmetrical positions along the LBD interface resulting in a stoichiometry of 2 modulator/dimer.¹¹

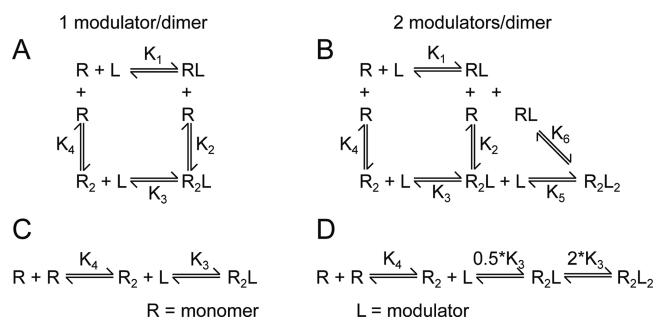


Figure 2. Cyclical and linear models for equilibrium dimerization are depicted for 1 modulator/dimer (A and C) and 2 modulators/dimer binding stoichiometries (B and D).

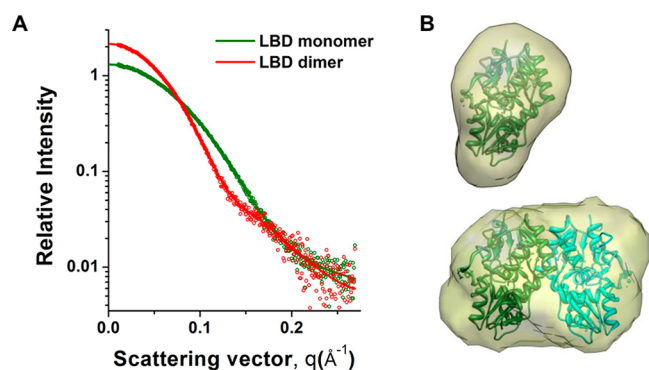


Figure 3. SAXS data (circles) (A) collected for the GluA2 LBD monomer and the L483Y constitutive dimer. The protein concentration was 0.1 mM in terms of the monomer. Idealized curves (thick lines) (A) were used to generate *ab initio* models (B) with DAMMIF.¹⁶ The monomeric [PDB: 1FTJ, chain A] and dimeric [PDB: 1FTJ, chains A,C] LBD structures⁴ were fit into surfaces for the respective models.

One copy of HFMZ was shown to bind to the dimer interface supporting a 1 modulator/dimer stoichiometry. The volume fraction of dimer for each sample mixture was extracted by determining the monomer and dimer components of the best fit to the SAXS data. The fraction of dimer was screened at various modulator and protein concentrations. The highest modulator concentration was bounded by its solubility limit. In addition, the protein concentrations were limited by solubility at high concentrations and resolution at low concentrations. Nonetheless, our SAXS measurements covered a large extent of

modulator and protein combinations for which the fraction of dimer was determined (Figure 4A–C and Supporting Information (SI) Figures S1 and S2) and allowed for curve fitting to equilibrium model-based equations.

Equations based on the cyclical models shown in Figure 2 were derived that could fit GluA2 LBD dimerization in terms of modulator concentration (e.g., SI Equation S24 for HFMZ). The equations are dependent on the protein concentration and fitting is required for a number of equilibrium constants. From the principle of detailed balance, the 1 modulator/dimer model equation required 3 unique equilibrium constants, while the 2 modulator/dimer model equation had 4 unique constants. An initial fitting of HFMZ-dependent dimerization was in good agreement with the 1 modulator/dimer model (Figure 4A) while the same equation was unable to fit the CYTZ-dependent dimerization (Figure 4B). Because the SAXS data sets are limited in coverage, the fitting of 4 equilibrium constants of the 2 modulator/dimer model equation could not be uniquely determined. The equation can be simplified (reduced to 3 unique equilibrium constants) if each modulator is assumed to bind to the dimer (R_2) with identical intrinsic K_D values and no cooperativity. This assumption is reasonable considering that allosteric modulators induce only minimal changes to the crystal structures of the GluA2 LBD, which is also a dimer in almost all crystals lacking modulators.¹⁷ In addition, both equations were simplified to a single preferred pathway from the cyclical models. In the simplified models, dimerization was reasoned to be the observed initial step followed by stabilization by modulator binding (Figures 2C and D). The detailed rationale is given in the supplementary data, but the

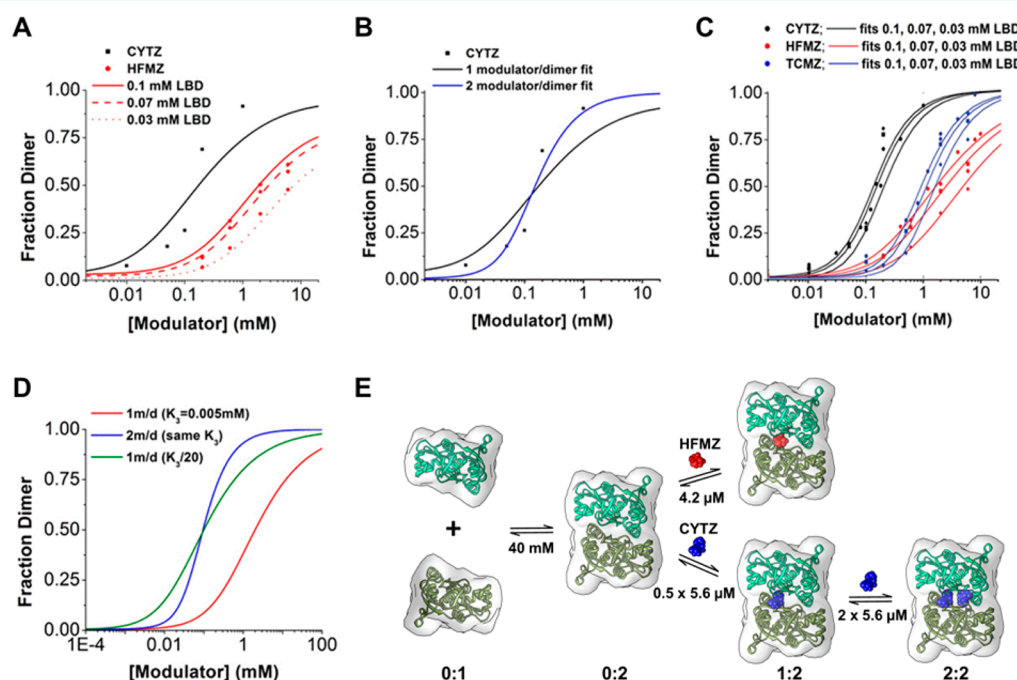


Figure 4. SAXS data and curve fitting for equilibrium dimerization models. (A) Fraction of dimer in the presence of CYTZ and HFMZ fit to the 1 monomer/dimer binding model. (B) Comparison between 1 and 2 monomer/dimer binding model fits for CYTZ-dependent dimerization. (C) The fraction of LBD dimer for CYTZ, HFMZ, and TCMZ at various protein concentrations were determined using SAXS and were fit simultaneously using equations derived from equilibrium dimerization models and the dissociation constants listed in (E) and (TCMZ, $K_3 = 46.8 \mu\text{M}$). (D) Hypothetical curves based on 1 modulator/dimer binding and 2 modulator/dimer binding with identical modulator EC_{50} values illustrate the shift in the EC_{50} of dimerization as well as the difference in apparent cooperativity. The 1 modulator/dimer binding model requires a 20-fold increase in modulator affinity to the dimer to achieve a similar EC_{50} as the 2 modulator/dimer binding model. (E) The modeled pathway for HFMZ-dependent dimerization and CYTZ-dependent dimerization is summarized.

affinity for modulator binding to the dimer would need to be several orders of magnitude higher than binding to the monomer for the data to fit (SI Figure S5). Dimerization induced by CYTZ and TCMZ can be fit better with a 2 modulator/dimer equation (SI Equation S14) while that for HFMZ can be fit better with a 1 modulator/dimer equation (SI Equation S6), supporting the modulator stoichiometry that was suggested by NMR spectroscopy and X-ray crystal structures (Figure 4C).¹¹ A striking difference is the apparent positive cooperativity that is exhibited when a second dimer-stabilizing modulator binding site is present.

The EC_{50} for dimerization by CYTZ (0.1–0.2 mM) is 10 \times lower than for TCMZ (1–2 mM) and 20 \times lower than for HFMZ (2–5 mM). These constants are given as a range because they vary with LBD concentration and would decrease further with increasing LBD concentration. Although EC_{50} values can be determined from dimerization curves, the values are dependent upon LBD concentration and are not directly relevant to the full GluA2 receptor. However, the dimerization curves are of value in two ways. First, the effect of one modulator relative to others is reflected in these curves. For example, in the intact receptor, as observed in the dimerization curves, HFMZ is considerably less potent than CYTZ. Second, microscopic constants can be extracted that are relevant to the action of these compounds. Using the linear models in Figures 2C and D (SI Equations S6 and S14), data from multiple SAXS experiments and protein concentrations for all three modulators were fit simultaneously to a one (HFMZ) or two site (CYTZ, TCMZ) models (Figure 4C and E). It should be noted that CYTZ represents a mixture of four diastereomeric racemates¹⁸ so the most important CYTZ species may have a much higher binding affinity than we report here, nonetheless the equilibrium constants are for the racemic CYTZ mixture that has been extensively used in iGluR electrophysiology studies. The intrinsic K_D (K_3) values for CYTZ and TCMZ binding to the dimer show the same 10-fold difference as the EC_{50} for dimerization ($\sim 5 \mu\text{M}$ and $50 \mu\text{M}$, respectively). Interestingly, K_3 values for CYTZ and HFMZ are roughly identical (both $\sim 5 \mu\text{M}$) although the EC_{50} for dimerization is 20 \times lower for CYTZ than for HFMZ. EC_{50} values for modulator binding to the dimer are comparable to values found previously for other thiazides (BPAM-97, $\sim 5 \mu\text{M}$; IDRA-21, $\sim 460 \mu\text{M}$) binding to the constitutive (L483Y) LBD dimer using isothermal titration calorimetry (ITC).¹⁹

To clarify the impact of the second modulator binding site, we generated dimerization curves for the simplified linear models with fixed parameters. For equilibrium dimerization models with identical K_3 values of modulator binding to the dimer, a decrease in the EC_{50} for dimerization and an increase in positive cooperativity is observed when a second binding site is present (Figure 4D). In order for the 1 modulator/dimer model to achieve a similar EC_{50} for dimerization as the 2 modulator/dimer model, the modulator binding affinity to the dimer needs to be 20 \times higher. Since dimer stabilization can be correlated with activation, it is an important determinant for modulator efficacy. The increased apparent dimerization constant imparted by adding a second equivalent binding site is of significant importance to development of allosteric regulators, and is expected to be present in the intact receptor as well as the LBD (see SI). A comparison of 1 and 2 binding site models illustrates why the stoichiometry of dimer-stabilizing modulators should be considered in rational drug design.

Current efforts are being directed at designing new GluA allosteric modulators for their use as cognitive enhancers. Efforts have focused on improving the affinity of lead compounds that bind to the full extent of the dimer interface with a 1 modulator/dimer stoichiometry, in some cases using the properties of thiazides with 2 modulator/dimer stoichiometry.^{9,20} A few studies have been directed toward building thiazides with increased effectiveness while maintaining the 2 modulator/dimer stoichiometry.^{9,21} While tethering 2 thiazides together in a way that maintains all modulator-LBD interactions could result in a significant improvement in affinity, there are a number of issues with this design strategy. The design of a compound with the correct geometries to maintain all of the bound interactions is a large challenge. In addition, larger drugs may have limited access to the dimer interfaces, and for receptors in the brain, size can be a limiting factor in crossing the blood–brain barrier.⁹ The results of our study suggest that the loss of a binding site because of obstruction by new steric constraints from the initial binding event should be avoided in GluA drug design and suggest that more effort in thiazide design could prove useful in cognitive enhancer development.

The conclusions of this work can be extended to the full glutamate receptor. If dimerization is the equivalent of receptor isomerization from an inactivated state to an activated state, then we can formulate similar equilibrium models and equations (SI Equations S2 and S9). The major difference between the models used for the LBD and the full receptor is the lack of protein concentration dependence for formation of the dimeric state. Since stabilization of the activated state can be achieved by the initial modulator binding event, adding a second equivalent binding event should result in an increase in modulator efficacy and in an apparent positive cooperativity.

Recently, a comprehensive three-body binding equilibrium model was developed and shown to describe existing experimental data that is tailored to cases in which two proteins are forced to interact through a dimerizing ligand (i.e., when the dimerization constant is low relative to the binding affinity of ligand for monomers).²² The result is an apparent autoinhibition at high dimerizing ligand concentrations because the ligand binds to both monomers and prevents three-body complex formation. Understanding the resulting autoinhibition is important for proteins that do not normally interact. Although we have focused on the binding to preformed dimers, we cannot rule out some binding to the monomeric state. In the case of binding to the monomeric state (particularly in the case of the one binding site modulators), an autoinhibition may be possible at high modulator concentrations (SI Figure S5). Our work provides insight into weak PPIs, which play a significant role in signaling and conformational dynamics.¹ Stabilization of these PPIs subsequently stabilizes transient conformational states, which are increasingly being recognized as important allosteric targets. Stoichiometric considerations in drug design can easily be translated to other allosteric targets. In exploring allosteric modulator stoichiometry, we have expanded our understanding of the principles that underlie dimer stabilization, which should be of direct relevance to medicinal chemistry.

METHODS

Materials and GluA2 LBD Purification. HFMZ and TCMZ were purchased from Sigma-Aldrich. CYTZ was purchased from Tocris Biosciences. The GluA2 LBD construct (S1S2J) was obtained from

Eric Gouaux. As previously described,¹¹ the construct consists of residues N392-K506 and P632-S775 of the rat GluA2-flop subunit (UniProtKB: P19491) with the N754S mutation, a 'GA' segment at the N-terminus, and a 'GT' linker connecting K506 and P632.⁴ Protein was obtained using standard *Escherichia coli* Origami B(DE3) protocols for the GluA2 LBD construct.¹¹ The protein was purified with an HT-SP ion exchange Sepharose column (Amersham Pharmacia) and a sizing column (Superose 12, XK26/100) after trypsin-cleavage of the 6-histidine tag.

Small Angle X-ray Scattering. The GluA2 LBD protein was exchanged into SAXS buffer (10 mM glutamate, 25 mM NaCl, 25 mM Tris-Cl, pH7) and concentrated to 3 mg mL⁻¹ (0.1 mM). Protein was diluted to the appropriate concentration (0.017 to 0.1 mM) with SAXS buffer. CYTZ, HFMZ, and TCMZ were solubilized in dimethyl sulfoxide (DMSO) and further diluted to the appropriate concentration with additional DMSO. The final samples consisted of 29 μ L of diluted protein and 1 μ L of diluted modulator stock. All SAXS experiments were collected at the Cornell High-Energy Synchrotron Source (CHESS)'s F2 beamline using a dual Pilatus 100K-S SAXS/WAXS detector. The 30 μ L samples were centrifuged at 14K rpm for 10 min before being loaded into a 96 well-plate. Capillary cells were robotically loaded with samples.²³ The samples were maintained at 4 °C on the plate until sample loading. Between each sample, the capillary cell was thoroughly washed with detergent and water and then dried with air. Background samples were taken in SAXS buffer only with all diluted modulator stocks. Protein samples without modulator included 1 μ L of DMSO. Background subtraction and data analysis were performed using the free open-source software, RAW.²³ The fraction of dimer in the modulator-protein mixtures was determined from SAXS data using the Oligomer program from the ATSAS suite.¹⁶ Data were fit using form factors from theoretical CRY SOL¹⁶-derived curves based on monomeric [PDB: 1FTJ, chain A] and dimeric [PDB: 1FTJ, chain A,C] GluA2 LBD.⁴

Equilibrium Binding Models. To obtain K_3 and K_4 values, the SAXS data sets for all modulators were fit simultaneously to SI Equations S6 and S14. Derivation of the fitting equations along with additional details can be found in the Supporting Information.

■ ASSOCIATED CONTENT

■ Supporting Information

Experimental procedures, derivation of equations, and additional data. This material is available free of charge via the Internet at <http://pubs.acs.org>.

■ AUTHOR INFORMATION

Corresponding Author

*Tel.: (607) 253-3650. Fax: (607) 253-3659. E-mail: reol@cornell.edu.

Notes

The authors declare no competing financial interest.

■ ACKNOWLEDGMENTS

This work was supported by grants from the National Institutes of Health (NIH) (R01-GM068935 and R21-NS067562) to R.E.O. It is based upon research conducted at the Cornell High Energy Synchrotron Source (CHESS). CHESS is supported by the National Science Foundation (NSF) and NIH/NIGMS via NSF award No. DMR-0936384, and the MacCHESS resource is supported by NIGMS award GM-103485. We thank R. Gillilan for assistance with BioSAXS data collection and analysis at the F2 beamline's dual Pilatus 100K-S SAXS/WAXS detector. We thank L. Nowak (Cornell), A. Loh (Univ. Wisc. LaCrosse), and B. Oswald (Applied Materials) for helpful discussions and L. Healy (Cornell) for participation in SAXS data collection.

■ REFERENCES

- (1) Nishi, H., Hashimoto, K., Madej, T., and Panchenko, A. R. (2013) Evolutionary, physicochemical, and functional mechanisms of protein homo-oligomerization. *Prog. Mol. Biol. Transl. Sci.* 117, 3–24.
- (2) Fegan, A., White, B., Carlson, J. C. T., and Wagner, C. R. (2010) Chemically controlled protein assembly: Techniques and applications. *Chem. Rev.* 110, 3315–3336.
- (3) Dubrovskaya, A., Kim, C., Elliott, J., Shen, W. J., Kuo, T. H., Koo, D. I., Li, C., Tuntland, T., Chang, J., Groessl, T., Wu, X., Gorney, V., Ramirez-Montagut, T., Spiegel, D. A., Cho, C. Y., and Schultz, P. G. (2011) A chemically induced vaccine strategy for prostate cancer. *ACS Chem. Biol.* 6, 1223–1231.
- (4) Armstrong, N., and Gouaux, E. (2000) Mechanisms for activation and antagonism of an AMPA-sensitive glutamate receptor: Crystal structures of the GluR2 ligand binding core. *Neuron* 28, 165–181.
- (5) Sun, Y., Olson, R., Horning, M., Armstrong, N., Mayer, M., and Gouaux, E. (2002) Mechanism of glutamate receptor desensitization. *Nature* 417, 245–253.
- (6) Sobolevsky, A. I., Rosconi, M. P., and Gouaux, E. (2009) X-ray structure, symmetry, and mechanism of an AMPA-subtype glutamate receptor. *Nature* 462, 745–756.
- (7) Trussell, L. O., and Fischbach, G. D. (1989) Glutamate receptor desensitization and its role in synaptic transmission. *Neuron* 3, 209–218.
- (8) Ward, S. E., Bax, B. D., and Harries, M. (2010) Challenges for and current status of research into positive modulators of AMPA receptors. *Br. J. Pharmacol.* 160, 181–190.
- (9) Pirotte, B., Francotte, P., Goffin, E., and de Tullio, P. (2013) AMPA receptor positive allosteric modulators: A patent review. *Expert Opin. Ther. Pat.* 23, 615–628.
- (10) Silverman, J. L., Oliver, C. F., Karras, M. N., Gastrell, P. T., and Crawley, J. N. (2013) AMPAKINE enhancement of social interaction in the BTBR mouse model of autism. *Neuropharmacology* 64, 268–282.
- (11) Ptak, C. P., Ahmed, A. H., and Oswald, R. E. (2009) Probing the allosteric modulator binding site of GluR2 with thiazide derivatives. *Biochemistry* 48, 8594–8602.
- (12) Jin, R. S., Clark, S., Weeks, A. M., Dudman, J. T., Gouaux, E., and Partin, K. M. (2005) Mechanism of positive allosteric modulators acting on AMPA receptors. *J. Neurosci.* 25, 9027–9036.
- (13) Ahmed, A. H., Ptak, C. P., and Oswald, R. E. (2010) Molecular Mechanism of Flop Selectivity and Subsite recognition for an AMPA receptor allosteric modulator: Structures of GluA2 and GluA3 in complexes with PEPA. *Biochemistry* 49, 2843–2850.
- (14) Rambo, R. P., and Tainer, J. A. (2010) Bridging the solution divide: Comprehensive structural analyses of dynamic RNA, DNA, and protein assemblies by small-angle X-ray scattering. *Curr. Opin. Struct. Biol.* 20, 128–137.
- (15) Madden, D. R., Armstrong, N., Svergun, D., Perez, J., and Vachette, P. (2005) Solution X-ray scattering evidence for agonist- and antagonist-induced modulation of cleft closure in a glutamate receptor ligand-binding domain. *J. Biol. Chem.* 280, 23637–23642.
- (16) Petoukhov, M. V., Franke, D., Shkumatov, A. V., Tria, G., Kikhney, A. G., Gajda, M., Gorba, C., Mertens, H. D. T., Konarev, P. V., and Svergun, D. I. (2012) New developments in the ATSAS program package for small-angle scattering data analysis. *J. Appl. Crystallogr.* 45, 342–350.
- (17) Pohlsgaard, J., Frydenvang, K., Madsen, U., and Kastrup, J. S. (2011) Lessons from more than 80 structures of the GluA2 ligand-binding domain in complex with agonists, antagonists, and allosteric modulators. *Neuropharmacology* 60, 135–150.
- (18) Cordi, A. A., Serkiz, B., Hennig, P., Mahieu, J. P., Bobichon, C., Denanteuil, G., and Lepagnol, J. M. (1994) Identification and characterization of the isomers of cyclothiazide responsible for potentiating AMPA current. *Bioorg. Med. Chem. Lett.* 4, 1957–1960.
- (19) Krintel, C., Frydenvang, K., Olsen, L., Kristensen, M. T., de Barrios, O., Naur, P., Francotte, P., Pirotte, B., Gajhede, M., and Kastrup, J. S. (2012) Thermodynamics and structural analysis of

positive allosteric modulation of the ionotropic glutamate receptor GluA2. *Biochem. J.* 441, 173–178.

(20) Dintilhac, G., Lan, D. A., Dilly, S., Danober, L., Botez, L., Lestage, P., Pirotte, B., and de Tullio, P. (2011) New substituted aryl esters and aryl amides of 3,4-dihydro-2H-1,2,4-benzothiadiazine 1,1-dioxides as positive allosteric modulators of AMPA receptors. *MedChemComm* 2, 509–523.

(21) Battisti, U. M., Jozwiak, K., Cannazza, G., Puia, G., Stocca, G., Braghiroli, D., Parenti, C., Brasili, L., Carrozzo, M. M., Citti, C., and Troisi, L. (2012) 5-Arylbenzothiadiazine type compounds as positive allosteric modulators of AMPA/kainate receptors. *ACS Med. Chem. Lett.* 3, 25–29.

(22) Douglass, E. F., Miller, C. J., Sparer, G., Shapiro, H., and Spiegel, D. A. (2013) A comprehensive mathematical model for three-body binding equilibria. *J. Am. Chem. Soc.* 135, 6092–6099.

(23) Nielsen, S. S., Moller, M., and Gillilan, R. E. (2012) High-throughput biological small-angle X-ray scattering with a robotically loaded capillary cell. *J. Appl. Crystallogr.* 45, 213–223.